MicroRNA-101 inhibits renal tubular epithelial-to-mesenchymal transition by targeting TGF-β1 type I receptor

QINGLAN WANG[1-3], YANYAN TAO[1], HONGDONG XIE[1], CHENGHAI LIU[1,2] and PING LIU[1,2]

[1]Institute of Liver Diseases, Shuguang Hospital Affiliated to Shanghai University of Traditional Chinese Medicine; [2]E-Institute of Shanghai Municipal Education Committee, [3]College of Basic Medical Science, Shanghai University of Traditional Chinese Medicine, Shanghai 201203, P.R. China

Received July 11, 2020; Accepted March 30, 2021

DOI: 10.3892/ijmm.2021.4952

Abstract. MicroRNAs (miRNAs/miRs) are key regulators of renal interstitial fibrosis (RIF). The present study was designed to identify miRNAs associated with the development of RIF, and to explore the ability of these identified miRNAs to modulate the renal tubular epithelial-to-mesenchymal transition (EMT) process. To this end, miRNAs that were differentially expressed between normal and fibrotic kidneys in a rat model of mercury chloride ($HgCl_2$)-induced RIF were detected via an array-based approach. Bioinformatics analyses revealed that miR-101 was the miRNA that was most significantly downregulated in the fibrotic renal tissue samples, and this was confirmed by RT-qPCR, which also demonstrated that this miRNA was downregulated in transforming growth factor (TGF)-β1-treated human proximal tubular epithelial (HK-2) cells. When miR-101 was overexpressed, this was sufficient to reverse TGF-β1-induced EMT in HK-2 cells, leading to the upregulation of the epithelial marker, E-cadherin, and the downregulation of the mesenchymal marker, α-smooth muscle actin. By contrast, the downregulation of miR-101 using an inhibitor exerted the opposite effect. The overexpression of miR-101 also suppressed the expression of the miR-101 target gene, TGF-β1 type I receptor (TβR-I), and thereby impaired TGF-β1/Smad3 signaling, while the opposite was observed upon miR-101 inhibition. To further confirm the ability of miR-101 to modulate EMT, the HK-2 cells were treated with the TβR-I inhibitor, SB-431542, which significantly suppressed TGF-β1-induced EMT in these cells. Notably, miR-101 inhibition exerted a less pronounced effect upon EMT-related phenotypes in these TβR-I inhibitor-treated HK-2 cells, supporting a model wherein miR-101 inhibits TGF-β1-induced EMT by suppressing TβR-I expression. On the whole, the present study demonstrates that miR-101 is capable of inhibiting TGF-β1-induced tubular EMT by targeting TβR-I, suggesting that it may be an important regulator of RIF.

Correspondence to: Dr Chenghai Liu or Dr Ping Liu, Institute of Liver Diseases, Shuguang Hospital Affiliated to Shanghai University of Traditional Chinese Medicine, 528 Zhangheng Road, Pudong New Area, Shanghai 201203, P.R. China
E-mail: chenghailiu@hotmail.com
E-mail: liuliver@vip.sina.com

Abbreviations: α-SMA, α-smooth muscle actin; ANOVA, one-way analysis of variance; DMEM, Dulbecco's modified Eagle's medium; ECM, extracellular matrix; EMT, epithelial-to-mesenchymal transition; FBS, fetal bovine serum; FDR, false discovery rate; $HgCl_2$, mercury chloride; miRNAs/miRs, microRNAs; RIF, renal interstitial fibrosis; TβR-I, TGF-β1 type I receptor; TβR-II, TGF-β1 type II receptor; TGF-β1, transforming growth factor-β

Key words: microRNA-101, tubular epithelial-to-mesenchymal transition, renal interstitial fibrosis, TGF-β1 type I receptor

Introduction

Renal interstitial fibrosis (RIF) is a pathological process that is common to the majority of chronic kidney diseases, resulting in functional deterioration which is largely independent of the initial renal injury (1). RIF is characterized by abnormal interstitial extracellular matrix (ECM) deposition (2). While a number of detailed studies on the mechanistic basis for RIF have been published in recent years, the etiology of this condition has yet to be fully clarified.

MicroRNAs (miRNAs/miRs) are short non-coding RNAs, which can modulate gene expression by altering target mRNA stability and translation to control key physiological and pathological processes (3,4). Indeed, miRNA dysregulation has been linked to an array of different disease processes (5). Within the kidneys, specific miRNAs regulate development, homeostasis and normal physiology, while also regulating the onset of a range of renal diseases (6). As such, further studies elucidating the miRNAs that regulate the incidence of RIF have the potential to highlight novel approaches with which to prevent or treat this debilitating condition.

In the present study, a miRNA array-based approach was utilized to identify miRNAs that were differentially expressed between fibrotic and normal kidney tissues using a rat model of mercury chloride ($HgCl_2$)-induced RIF (7,8). This analysis identified miR-101 (also termed miR-101a, miR-101a-3p) as the miRNA that was the most significantly downregulated in fibrotic renal tissue. In previous studies, miR-101 has also been shown to be involved in fibrotic processes, such as liver fibrosis (9,10), pulmonary fibrosis (11), cardiac fibrosis (12,13),

bladder fibrosis (14) and cystic fibrosis (15). The role of this miRNA in the context of RIF, however, remains to be clarified, as do the molecular mechanisms underlying such a role. As such, the present study further evaluated the ability of miR-101 to regulate RIF.

One of the key steps in the development of RIF is renal tubular epithelial-to-mesenchymal transition (EMT), wherein tubular epithelial cells adopt a mesenchymal-like phenotype and lose their epithelial-like traits (16). The disruption of tubular EMT is thus a viable approach for the treatment of RIF (17,18). Transforming growth factor-β1 (TGF-β1) is an essential regulator of this renal tubular EMT process (19,20), signaling through its cognate cell-surface type I and II receptors (TβR-I and TβR-II, respectively) to induce appropriate downstream signaling pathway activation. There is prior evidence to indicate that TβR-I is a direct miR-101 target (21), and as such, it was hypothesized that miR-101 may be able to regulate renal tubular EMT by targeting TβR-I and thereby suppressing TGF-β1 signaling.

The present study thus examined the ability of miR-101 to reverse TGF-β1-induced tubular EMT in human proximal tubular epithelial (HK-2) cells. Through these analyses, it was determined that TGF-β1 treatment led to the downregulation of miR-101. In addition, miR-101 overexpression suppressed TGF-β1-induced EMT, whereas miR-101 knockdown exerted the opposite effect. At a mechanistic level, miR-101 suppressed TGF-β1 signaling by inhibiting TβR-I expression, and the blocking of TβR-I signaling ablated the effects of miR-101 inhibition on TGF-β1-induced EMT. Overall, the results thus demonstrated that miR-101 inhibited tubular EMT, at least in part by suppressing TβR-I expression.

Materials and methods

Rat model of $HgCl_2$-induced RIF. In total, 20 male Sprague-Dawley rats (4-5 weeks old, weighing 120±10 g) were obtained from the Shanghai Laboratory Animal Center, Chinese Academy of Sciences. All rats were housed in a specific pathogen-free environment that was maintained at 22-24˚C with a relative humidity of 50-60% and a 12-h light/dark cycle. All rats were provided with *ad libitum* access to food and water. These animals were then randomly divided into the control (n=8) and model (n=12) groups, with the animals in the latter group being orally administered with $HgCl_2$ (8 mg/kg; Shanghai Tongren Pharmaceutical Co., Ltd.) once daily for nine weeks. These experimental protocols were conducted in accordance with internationally accepted laboratory principles and all animals received humane care as well as free access to food and water. The present study was approved by The Animal Research Ethics Committee of Shanghai University of Traditional Chinese Medicine, Shanghai, China. The humane endpoint for this study was a loss of 15% of the starting body weight. The animals were anesthetized using 1% pentobarbital sodium (50 mg/kg) by intraperitoneal (i.p.) injection. The samples of blood (0.8 ml) were collected from the vena cava. After collecting the blood and kidney, at the end of the experimental procedure, the abdominal vasculature, including the vena cava was cut to cause exsanguination under deep anesthesia. Death was further confirmed by checking for the onset of rigor mortis (22). The body weight was measured at the time of sacrifice, and body weight loss was not observed in any of the rats, with the body weight ranging from 331 to 492 g.

Cells, cell culture and treatment. HK-2 cells were obtained from the Institute of Basic Medical Sciences, Chinese Academy of Medical Sciences, and were grown in DMEM (Gibco; Thermo Fisher Scientific, Inc.) containing 10% fetal bovine serum (FBS, Gibco; Thermo Fisher Scientific, Inc.) for 18 h. Cells were then transferred to serum-free medium and were treated for 48 h with 5 ng/ml TGF-β1 to achieve EMT induction. In appropriate experiments, cells were transfected with 20 nM of miR-101 mimic (Guangzhou RiboBio Co., Ltd.; the mature sequence of hsa-miR-101 mimic was UACAGUACUGUGAUAACUGAA) or 50 nM of miR-101 inhibitor (Guangzhou RiboBio Co., Ltd.) or appropriate controls using a ribioFECT CP Transfection kit (Guangzhou RiboBio Co., Ltd.) along with 5 ng/ml TGF-β1 for 48 h. In order to assess how TβR-I affects these results, in appropriate experiments, cells were treated with 10 μM of SB-431542 (Tocris Bioscience) to specifically inhibit TβR-I for 12 h, and the cells were then transfected with miR-101 inhibitor or appropriate controls using a ribioFECT CP Transfection kit (Guangzhou RiboBio Co., Ltd.) along with 5 ng/ml TGF-β1 or SB-431542 for a further 48 h.

Hydroxyproline measurements. Renal hydroxyproline levels were measured based upon HCl hydrolysis as per the method described in the study by Jamall *et al* (23). Briefly, 100 mg of renal tissue was homogenized in 2.5 ml of ice-cold ddH_2O, after which a BCA kit (Thermo Fisher Scientific, Inc.) was used to quantify the protein levels in these samples. Subsequently, 6 M HCl were used to hydrolyze 2 ml of these homogenates for 18 h at 105˚C, and the resultant hydrolysates were filtered using 3-mm filter paper prior to drying at 40˚C. Samples were then incubated with Ehrlich's solution [25% (w/v) p-dimethylaminobenzaldehyde and 27.3% (v/v) perchloric acid in isopropanol] at 50˚C for 1.5 h, followed by assessment at 558 nm using a Tecan Infinite M200 Pro plate reader (Tecan Life Sciences), with protein concentrations being used to normalize the resultant values.

Histological analysis. The kidney samples were fixed using 10% formalin, paraffin-embedded, and cut into 5-μM-thick sections. The sections were then subjected to Masson's trichrome staining using a modified Masson's Trichrome stain kit (Solarbio Science & Technology Co., Ltd.) according to the manufacturer's instructions. Briefly, the sections were stained in Harris hematoxylin for 5 min, in Ponceau acid fuchsin staining solution for 10 min, and in Aniline Blue solution for 5 min at room temperature. Hematoxylin and eosin (H&E) staining was performed using a H&E staining kit (Yeasen Biotech Co., Ltd.) according to the manufacturer's instructions. Briefly, the sections were stained in hematoxylin for 5 min and in eosin solution for 1 min at room temperature. Images were obtained using an Olympus IX73 microscope (Olympus Corporation). ImageJ software for Windows V 1.52v (NIH) was used to quantify the Masson's trichrome positive staining area.

miRNA microarray. Renal miRNA profiles in these animals (two samples in each group) were evaluated using an Agilent Rat microRNA Microarray 16.0 (Agilent Technologies. Inc.). Total renal tissue RNA was extracted using a mirVana™ miRNA Isolation kit (Ambion; Thermo Fisher Scientific, Inc.), after which an Agilent Bioanalyzer 2100 was used to assess the RNA quality based upon the RNA integrity number (RIN) statistic. The miRNAs in these samples were then labeled and hybridized with a miRNA Complete Labeling and Hyb kit (Agilent Technologies, Inc.) based on the provided directions, and the Agilent Microarray Scanner and Feature Extraction software (v10.7) was used to analyze these slides under default settings. The Quantile algorithm was used to normalize the resultant raw data with the Gene Spring Software v11.0 (Agilent Technologies, Inc.). Shanghai Biotechnology Corporation conducted these microarray analyses.

miRNA microarray analysis. Linear models and empirical Bayes methods were used to detect differentially expressed miRNAs (24), with the thresholds for differential expression being the following: $P<0.05$, false discovery rate (FDR) <0.05 and fold change (FC) >1.5.

TargetScan (http://www.targetscan.org) was used to identify putative miRNA target genes, with the resultant miRNA-gene network being constructed based upon the associations between these miRNAs and genes in the Sanger microRNA database (http://www.mirbase.org) and on the strength of their interactions. This network was constructed as an adjacency matrix $A=[a_{i,j}]$, where $a_{i,j}$ represents the relational weights of gene 'I' and microRNA 'j'. In the final network, squares and circles were used to represent miRNAs and mRNAs, respectively, with single edges being used to represent associations between miRNAs and target genes. Degree values were used to represent centrality within this network, indicating the contribution of one miRNA to the surrounding genes such that key miRNAs have larger degree values (25).

Reverse transcription-quantitative PCR (RT-qPCR). A Qiagen miRNeasy Mini kit (Qiagen, Inc.) was used to extract mRNA and miRNAs from the samples. Relative gene expression was analyzed using the $2^{-\Delta\Delta Cq}$ method (26), with U6 and β-actin being used to normalize miRNA and mRNA expression, respectively. A SYBR-Green Real-Time PCR kit (Takara Bio, Inc.) was used for qPCR with the following primers: Human E-cadherin forward, 5'-AAGACAAAGAAGGCAAGGTT-3' and reverse, 5'-AAGAGAGTGTATGTGGCAAT-3'; human α-smooth muscle actin (α-SMA) forward, 5'-GGACATCAAGGAGAAACTGT-3' and reverse, 5'-CCATCAGGCAACTCGTAACT-3'; human TβR-I forward, 5'-TGTGAAGCCTTGAGAGTAAT-3' and reverse, 5'-TGTTGACTGAGTTGCGATAA-3'; and β-actin forward, 5'-CACGATGGAGGGGCCGGACTCATC-3' and reverse, 5'-TAAAGACCTCTATGCCAACACAGT-3'. Primers for U6 and miRNA were from GeneCopoeia, Inc. The cycling conditions were as follows: 95˚C for 30 sec, followed by 40 cycles of 95˚C for 5 sec, and 60˚C for 10 sec.

Western blot analysis. RIPA buffer supplemented with a complete mini protease inhibitor cocktail and a PhosSTOP phosphatase inhibitor cocktail (Roche Diagnostics) was used to lyse the HK-2 cell and renal tissue samples, which were then spun for 15 min at 13,000 x g at 4˚C. A BCA assay (Thermo Fisher Scientific, Inc.) was then used to assess the protein quantities in the collected supernatants, and equal protein amounts (30 μg) were separated via 10% SDS-PAGE prior to transfer onto nitrocellulose membranes. Following a 1-h blocking step using 5% non-fat milk for 1 h at room temperature, these blots were probed overnight at 4˚C with primary anti-α-SMA (1:1,000, ab7817), anti-E-cadherin (1:1,000 ab40772), anti-Smad3 (1:1,000 ab40854), anti-p-Smad3 (1:500 ab52903), anti-TβR-I (1:1,000 ab31013) and anti-GAPDH antibodies (1:5,000 ab8245) (Abcam). The blots were then washed, incubated with secondary HRP-conjugated goat anti-mouse antibody (1:5,000, ab97023, Abcam) or goat anti-rabbit antibody (1:5,000, ab205718, Abcam) for 1 h at room temperature, and protein bands were then visualized using an ECL reagent (Thermo Fisher Scientific, Inc.), with a Tanon 5200 detection system (Tanon Science & Technology Co., Ltd.) being used for imaging. Protein band densitometry was quantified using ImageJ software for Windows V 1.52v (NIH) and normalized to GAPDH.

Immunofluorescence staining. E-cadherin and α-SMA expression was assessed via immunofluorescence in HK-2 cells by plating these cells in 96-well plates, washing them with PBS twice, and then fixing them using 4% paraformaldehyde. Subsequently, 5% BSA in PBS was used to block the cells for 30 min at room temperature, after which they were incubated with primary anti-α-SMA (1:200, ab7817; Abcam) and anti-E-cadherin (1:50, ab40772; Abcam) antibodies at room temperature for 1 h. Cy3-conjugated goat anti-rabbit secondary antibody (1:200, A10520; Thermo Fisher Scientific, Inc.) and FITC-conjugated goat anti-mouse secondary antibody (1:200, F2761; Thermo Fisher Scientific, Inc.) were then incubated with these cells for 1 h at 37˚C, after which Hoechst 33258 (Thermo Fisher Scientific, Inc.) was used for nuclear staining at room temperature for 5 min, and a Thermo Fisher Scientific ArrayScan HCS reader was used for image acquisition, with the Thermo HCS Studio™ 2.0 Cell Analysis Program was used for subsequent data analysis.

Statistical analysis. Data are presented as the mean ± SEM. GraphPad Prism 7 was used for all statistical analysis. Data were compared using Student's t-tests and one-way ANOVA with Tukey's post hoc analysis, as appropriate. $P<0.05$ was the significance threshold, and all experiments were repeated three or more times.

Results

$HgCl_2$ treatment induces renal inflammation and interstitial fibrosis. The present study first analyzed the H&E-stained kidney sections from the rats, revealing that $HgCl_2$ treatment was associated with renal tubular deformation and mononuclear cell infiltration. This was in sharp contrast to the normal glomerul'ar and tubular architecture observed in the control animals (Fig. 1A).

Collagen deposition is a key hallmark of tissue fibrosis, and can be evaluated via Masson's trichrome staining and by measuring hydroxyproline content. Masson's staining indicated that $HgCl_2$ treatment resulted in increased collagen

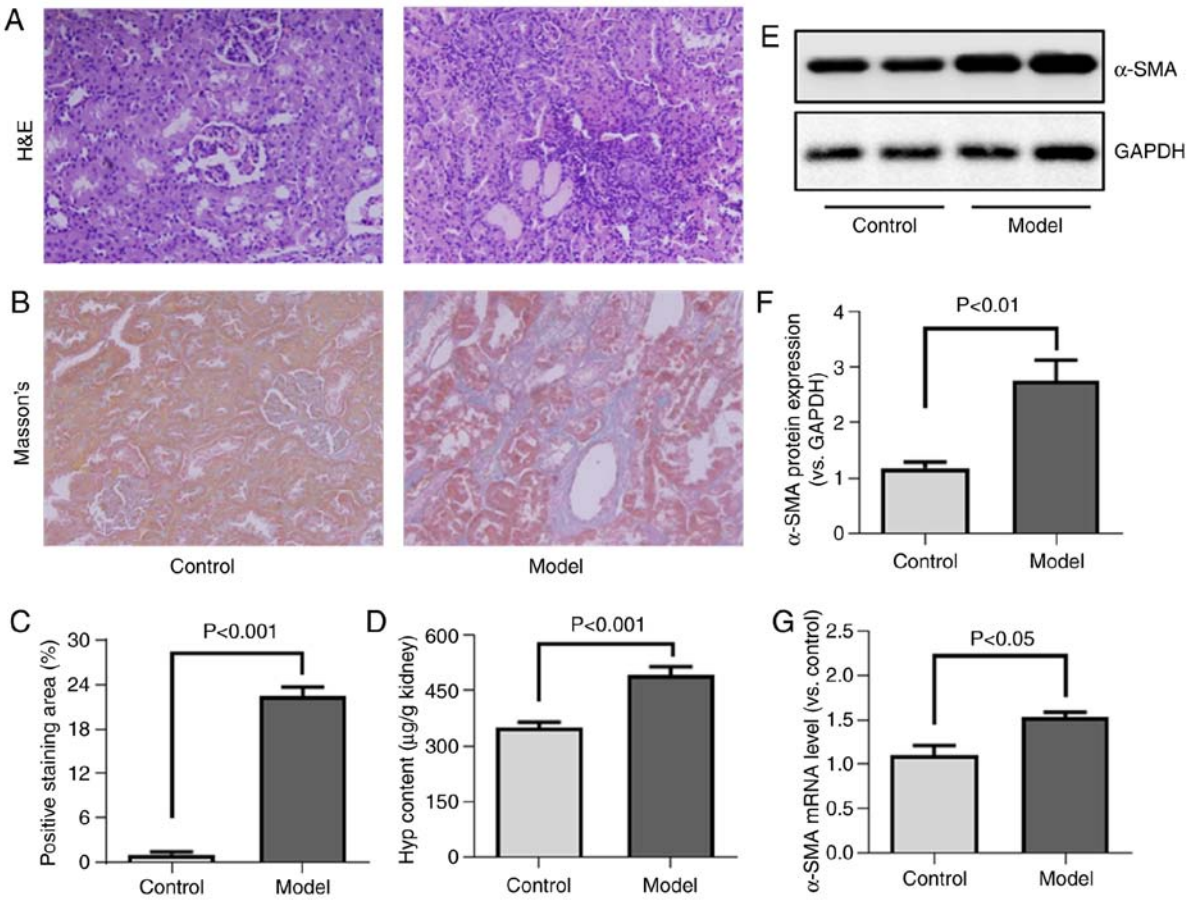

Figure 1. $HgCl_2$ induces renal inflammation and interstitial fibrosis in rats. (A) Representative H&E-stained renal tissues. (B) Representative Masson's trichrome-stained tissues used to analyze RIF. (C) Quantification of Masson's trichrome positive staining area in renal tissue samples. (D) Renal hydroxyproline levels were measured using the method by Jamall *et al* (23). (E) Renal α-SMA levels were assessed via western blot analysis. (F) α-SMA levels in western blots were quantified via densitometry and were normalized to GAPDH. (G) Renal α-SMA mRNA expression was assessed by RT-qPCR. $HgCl_2$, mercury chloride; RIF, renal interstitial fibrosis; α-SMA, α-smooth muscle actin; Hyp, hydroxyproline.

deposition (Fig. 1B and C). The renal hydroxyproline content was similarly elevated in the $HgCl_2$-treated rats compared with the controls (Fig. 1D).

α-SMA is a marker of ECM-secreting myofibroblasts, and it was found that $HgCl_2$ treatment significantly enhanced α-SMA expression at the protein and mRNA level (Fig. 1E-G), thus confirming that this treatment was linked to an enhanced renal myofibroblast activation.

Identification of key differentially expressed miRNAs associated with $HgCl_2$-induced RIF. Using an array-based approach, 40 miRNAs that were differentially expressed between the control and RIF model animals were identified, of which 17 and 23 were downregulated and upregulated, respectively (Fig. 2A). TargetScan was used to predict target genes for these miRNAs and a miRNA-gene network based upon predicted interactions among these miRNAs and genes was then constructed using the Sanger miRNA database (Fig. 2B). The degree metric was used to determine centrality within this network, reflecting the degree to which a given miRNA contributes to the regulation of the surrounding genes, with key miRNAs having a larger degree value (25). The top 10 most central miRNAs within this network included four downregulated miRNAs (miR-101a, miR-107, miR-194 and miR-142-3p, with respective degree values of 102, 63, 48 and 43) and six upregulated miRNAs (miR-27a, let-7i, miR-34a, miR-214, miR-199a-3p and miR-21, with respective degree values of 170, 126, 93, 76, 60 and 42) (Fig. 2C).

miR-101 is downregulated in fibrotic kidney tissue and TGF-β1-treated HK-2 cells. Given that miR-101 was among the most significantly downregulated miRNAs in the miRNA-mRNA network (Fig. 2C), the present study then explored the role of this miRNA in the context of RIF. First it was confirmed that miR-101 downregulation was evident in the $HgCl_2$-treated fibrotic kidney tissue by RT-qPCR, in line with the microarray findings (Fig. 3A).

Renal tubular EMT is a key driver of the development of RIF (27). The present study therefore explored this process *in vitro* by treating HK-2 cells with TGF-β1. Consistent with the successful EMT induction, TGF-β1 treatment resulted in both the loss of epithelial E-cadherin expression and the upregulation of mesenchymal α-SMA expression in HK-2 cells, as confirmed by western blot analysis (Fig. 3C-E). Additionally, miR-101 expression was assessed in these cells by RT-qPCR, and it was confirmed that this miRNA was downregulated in the context of TGF-β1-induced EMT (Fig. 3B).

miR-101 inhibits TGF-β1-induced EMT in HK-2 cells. HK-2 cells were then transfected with a miR-101 mimic or a

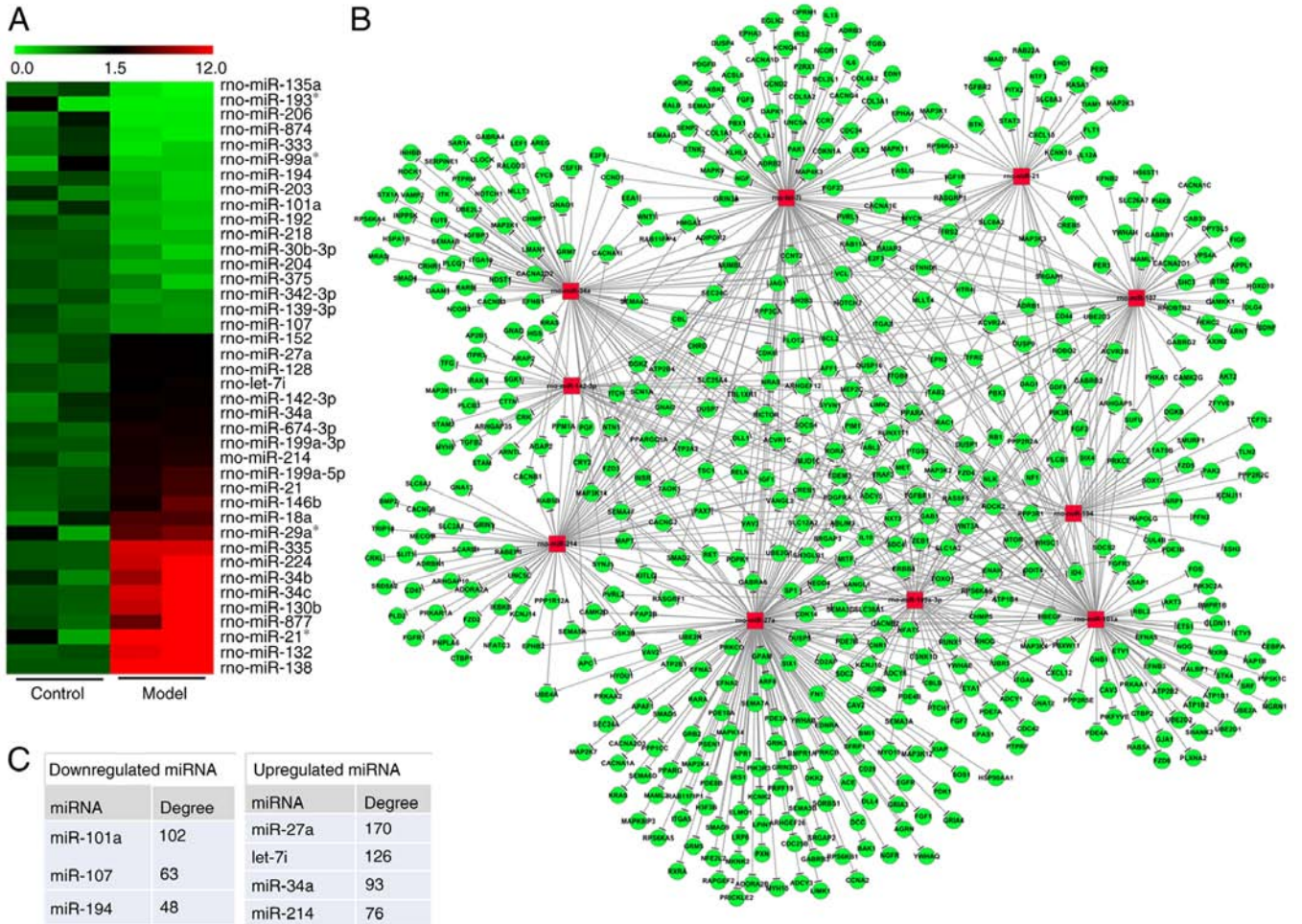

Downregulated miRNA	
miRNA	Degree
miR-101a	102
miR-107	63
miR-194	48
miR-142-3p	42

Upregulated miRNA	
miRNA	Degree
miR-27a	170
let-7i	126
miR-34a	93
miR-214	76
miR-199a-3p	60
miR-21	42

Figure 2. Identification of key differentially expressed miRNAs associated with $HgCl_2$-induced renal interstitial fibrosis. (A) Data from a miRNA microarray comparing expression levels between control and RIF model rats were arranged in a heatmap. The color scale indicates the expression level of the miRNA, with green and red colors indicating low and high expression, respectively. (B) A miRNA-gene network was constructed, with squares and circles corresponding to miRNAs and genes, respectively. Associations between these network elements are represented by edges, with network centrality corresponding to degree values. (C) The degree values for the 10 top miRNAs within this network, with miR-101 being identified as the most significant downregulated miRNA in this disease context. The red square represents miRNA and the green circle represents mRNA. $HgCl_2$, mercury chloride.

corresponding control construct, after which these cells were treated with TGF-β1. As was expected, miR-101 mimic transfection was associated with a significant increase in miR-101 expression, whereas TGF-β1 treatment decreased miR-101 expression (Fig. 4A).

When the effects of miR-101 on TGF-β1-induced EMT were evaluated in these HK-2 cells, it was found that miR-101 mimic transfection resulted in an increased E-cadherin expression at the protein (Fig. 4B-E) and mRNA (Fig. 4F) level, along with a decreased α-SMA protein (Fig. 4B-E) and mRNA (Fig. 4F) expression, consistent with the suppression of EMT in these cells.

miR-101 knockdown promotes TGF-β1-induced EMT in HK-2 cells. The present study then assessed the effects of miR-101 downregulation on TGF-β1-induced EMT in HK-2 cells by transfecting the cells with a miR-101 inhibitor prior to TGF-β1 treatment, resulting in a significant knockdown of miR-101 expression (Fig. 5A). This inhibition of miR-101 was associated with a significant decrease in E-cadherin protein (Fig. 5B, C, E and F) and mRNA (Fig. 5D) expression, while α-SMA protein (Fig. 5, C, E and F) and mRNA (Fig. 5D) expression increased significantly in these cells. These results thus revealed that miR-101 downregulation enhanced TGF-β1-induced EMT in these HK-2 cells.

Effect of miR-101 on TβR-I and Smad3 expression in HK-2 cells. Previous studies have identified TβR-I as a miR-101 target gene (21,28). The present study thus assessed the effects of miR-101 on TβR-I expression in the TGF-β1-treated HK-2 cells. This approach revealed that TGF-β1 treatment enhanced TβR-I expression, whereas miR-101 mimic transfection inhibited its expression (Fig. 6A and B). By contrast, transfection with miR-101 inhibitor was associated with an increased TβR-I expression in the TGF-β1-treated HK-2 cells (Fig. 6D and E).

The TGF-β1/Smad pathway serves to facilitate canonical TGF-β1 signaling within cells, with Smad3 phosphorylation being a key step in this pathway (29). The present study confirmed, by western blot analysis, that miR-101 mimic transfection was associated with a decreased Smad3

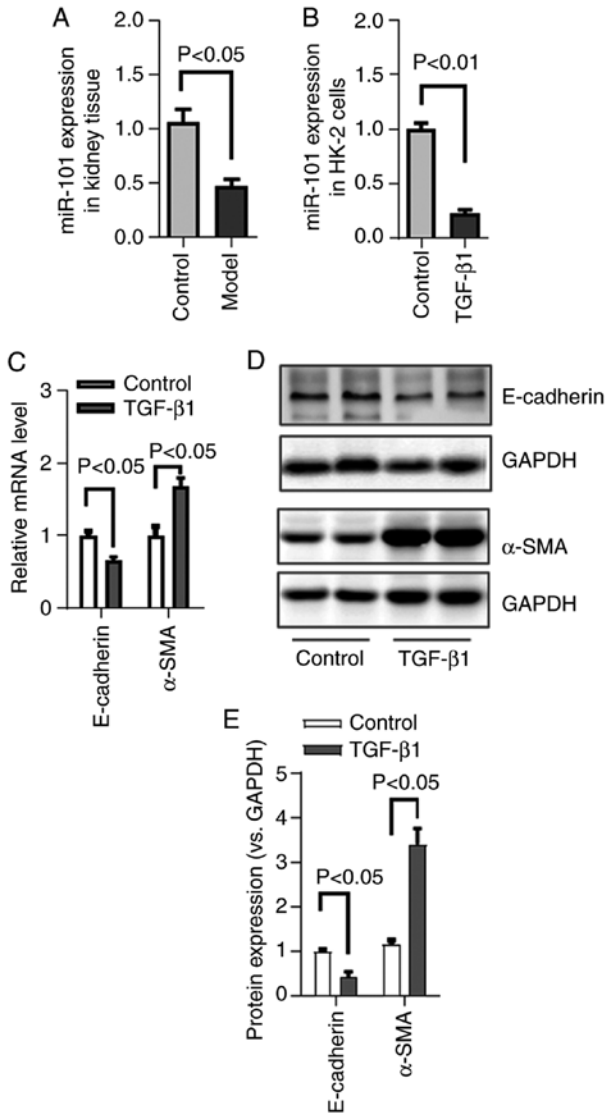

Figure 3. miR-101 downregulation is evident in both the RIF model renal tissue and TGF-β1 treated HK-2 cells. (A) RT-qPCR was used to assess miR-101 expression in renal tissues. (B) RT-qPCR was used to assess miR-101 expression in TGF-β1-treated HK-2 cells. (C) RT-qPCR was used to assess E-cadherin and α-SMA expression in TGF-β1-treated HK-2 cells. (D) Western blot analysis was used to assess E-cadherin and α-SMA protein. (E) Densitometric quantification of the results in (D), with GAPDH used for normalization. RIF, renal interstitial fibrosis; α-SMA, α-smooth muscle actin; TGF-β1, transforming growth factor-β1.

phosphorylation (Fig. 6A and C), whereas the inhibition of miR-101 exerted the opposite effect in TGF-β1-treated HK-2 cells (Fig. 6D and F).

TβR-I inhibition impairs TGF-β1-induced EMT and the effect of miR-101 inhibition on HK-2 cells. In an effort to more fully assess whether miR-101 targets TβR-I to suppress the EMT process in HK-2 cells, the present study then assessed whether the effect of miR-101 inhibitor transfection on EMT was disrupted when the cells were treated with the potent TβR-I inhibitor, SB-431542 (30). As was expected, SB-431542 markedly impaired TGF-β1-induced EMT in the HK-2 cells, enhancing E-cadherin expression and suppressing α-SMA expression (Fig. 7A and B). When the cells were treated with SB-431542, this ablated the effects of miR-101 inhibitor transfection on EMT-related phenotypes (Fig. 7A and B), indicating that miR-101 targets TβR-I to inhibit TGF-β1-induced EMT. When TβR-I protein expression was assessed, it was confirmed that SB-431542 treatment markedly decreased TβR-I protein expression, whereas miR-101 inhibitor treatment did not further affect the TβR-I protein levels in these SB-431542-treated HK-2 cells (Fig. 7C and D).

Discussion

A number of studies to date have highlighted the roles played by miRNAs in the context of both pathological and physiological processes (5). Specific miRNAs have been found to regulate renal development, homeostasis and the pathology of RIF as well as other diseases (6,31). While the general etiology of RIF has been thoroughly studied, the specific regulatory roles of individual miRNAs in this disease context remain to be fully elucidated. By further studying the ability of these miRNAs to influence RIF progression, it may be possible to identify novel approaches to preventing or treating this condition.

Herein, a previously described $HgCl_2$-induced rat model of RIF was employed (8,32). By analyzing renal tissues from these animals, 17 and 23 miRNAs were identified that were downregulated and upregulated, respectively, in fibrotic kidney tissue samples relative to the control kidney samples. Through bioinformatics analyses, the 10 most critical of these miRNAs were then identified, including four that were downregulated (miR-101, miR-107, miR-194 and miR-142-3p) and six that were upregulated (miR-27a, let-7i, miR-34a, miR-214, miR-199a-3p and miR-21) in fibrotic renal tissue. The majority of these miRNAs have previously been linked to renal diseases, such as RIF. For example, Hou *et al* (33) found miR-27a to suppress peroxisome proliferator-activated receptor-γ signaling and to thereby promote RIF, whereas miR-34a has been shown to regulate Klotho expression in tubular epithelial cells, thereby controlling RIF (34), while also inducing the apoptotic death of these cells (35). There is also evidence to indicate that miR-214 is upregulated in the context of renal injury, and the knockdown of this miRNA is sufficient to attenuate unilateral ureteral obstruction (UUO)-induced RIF (36). miR-21 is among the most well-characterized miRNAs associated with fibrosis in a range of tissue types (37-39). In healthy renal tissue, minimal miR-21 expression is observed, whereas it is significantly upregulated in the context of RIF, wherein it can target PTEN and peroxisome proliferator-activated receptor-α to promote fibrotic progression (38). These findings thus confirm that HgCl2 induces a model of RIF similar to that induced by a UUO-based approach, while also confirming the reliability of our miRNA array findings.

Using bioinformatics analyses, the present study identified miR-101 as the most downregulated miRNA in the rat model of $HgCl_2$-induced RIF. This miRNA has previously been reported to play roles in other fibrotic processes, including liver fibrosis (9,10), pulmonary fibrosis (11), cardiac fibrosis (12,13), bladder fibrosis (14) and cystic fibrosis (15); however, its importance in the context of RIF has not been well-characterized. As such, the present study explored its role in this pathological setting. Renal tubular EMT is a key step in RIF progression (40), and is characterized by tubular cells undergoing a shift from an epithelial-like to a mesenchymal-like phenotype, whereupon

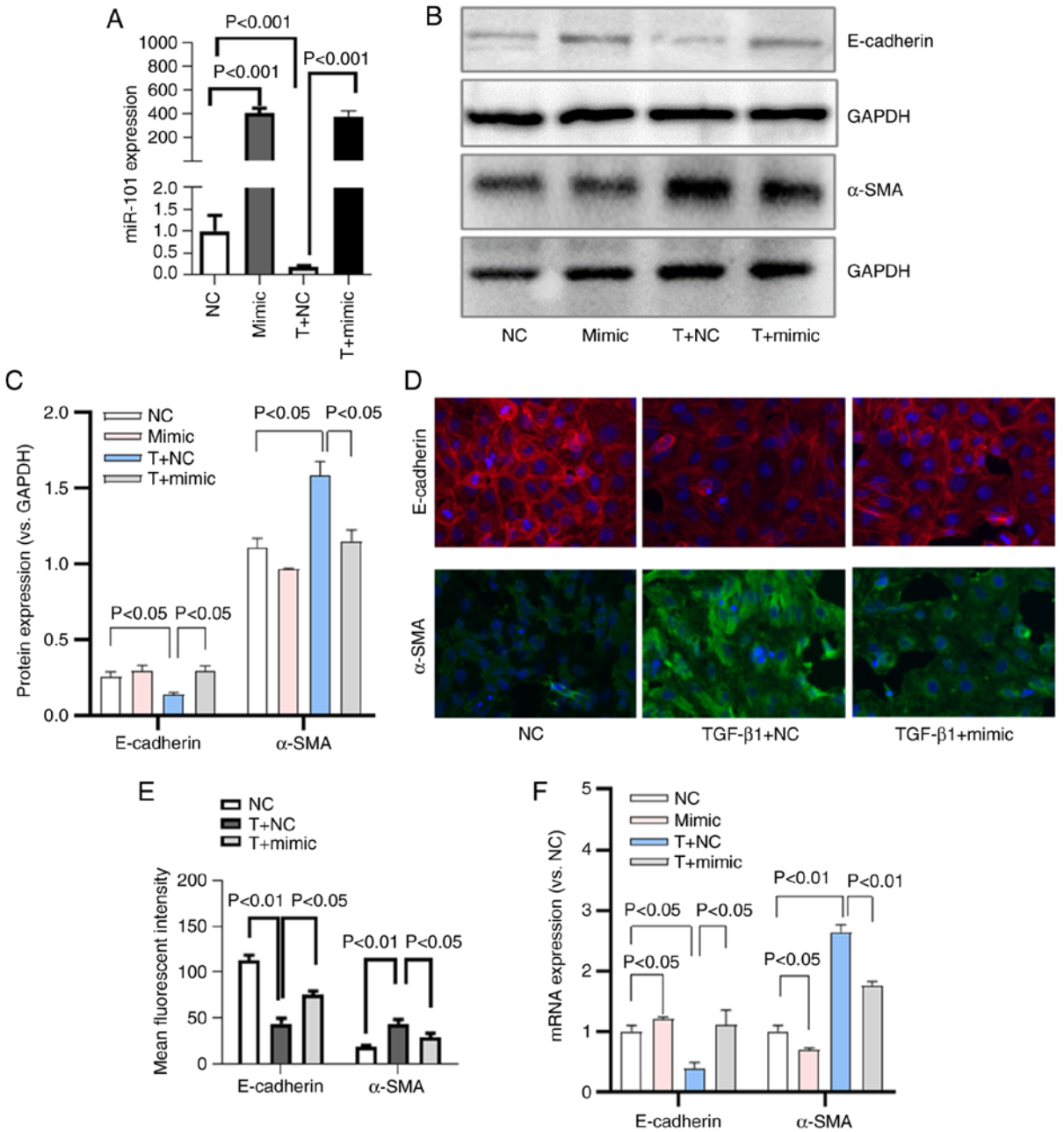

Figure 4. miR-101 inhibits TGF-β1-induced EMT in HK-2 cells. (A) miR-101 expression was quantified in HK-2 cells. (B) Levels of E-cadherin and α-SMA in HK-2 cells were measured by western blot analysis. (C) Densitometric quantification of data in (B), with GAPDH used for normalization. (D) E-cadherin and α-SMA expression as assessed by immunofluorescence. (E) E-cadherin and α-SMA staining intensity was quantified using the Thermo HCS StudioTM 2.0 Cell Analysis Program. (F) RT-qPCR was used to assess E-cadherin and α-SMA mRNA expression. NC, negative control; T, TGF-β1; mimic, miR-101 mimic; EMT, epithelial-to-mesenchymal transition; α-SMA, α-smooth muscle actin; TGF-β1, transforming growth factor-β1.

these cells are able to produce high levels of ECM components and to thereby drive RIF pathogenesis (8). TGF-β1 is the most well-studied inducer of EMT (41), which is also downregulated in HgCl2-induced RIF (8,32), and as such, this was utilized in the present study to induce this process in HK-2 cells. In line with the findings *in vivo*, a reduced miR-101 expression was observed in the cells following TGF-β1 treatment. When miR-101 was overexpressed in these same cells, it was found that this reversed TGF-β1-induced EMT, whereas miR-101 inhibition exerted the opposite effect. Taken together, these findings highlight miR-101 as an inhibitor of tubular EMT.

The TGF-β1/Smad pathway is an essential mediator of EMT progression that is initiated upon the binding of TGF-β1 to the cell surface TβR-II molecule, in turn resulting in TβR-I activation, Smad2/3 phosphorylation and nuclear translocation and altered gene expression. Previous research has demonstrated that miR-101 can suppress fibrosis owing to its ability to target TβR-I and to thereby suppress TGF-β1 signaling (21). In line with this finding, the present study determined that miR-101 was able to inhibit EMT progression via downregulating TβR-I, as miR-101 overexpression disrupted TGF-β1-induced TβR-I mRNA and protein expression. The TGF-β1/Smad pathway is an essential mediator of canonical TGF-β1 signaling (29), with Smad3 phosphorylation being a key component of this process. Consistently, it was determined that miR-101 was able to inhibit TGF-β1-induced Smad3

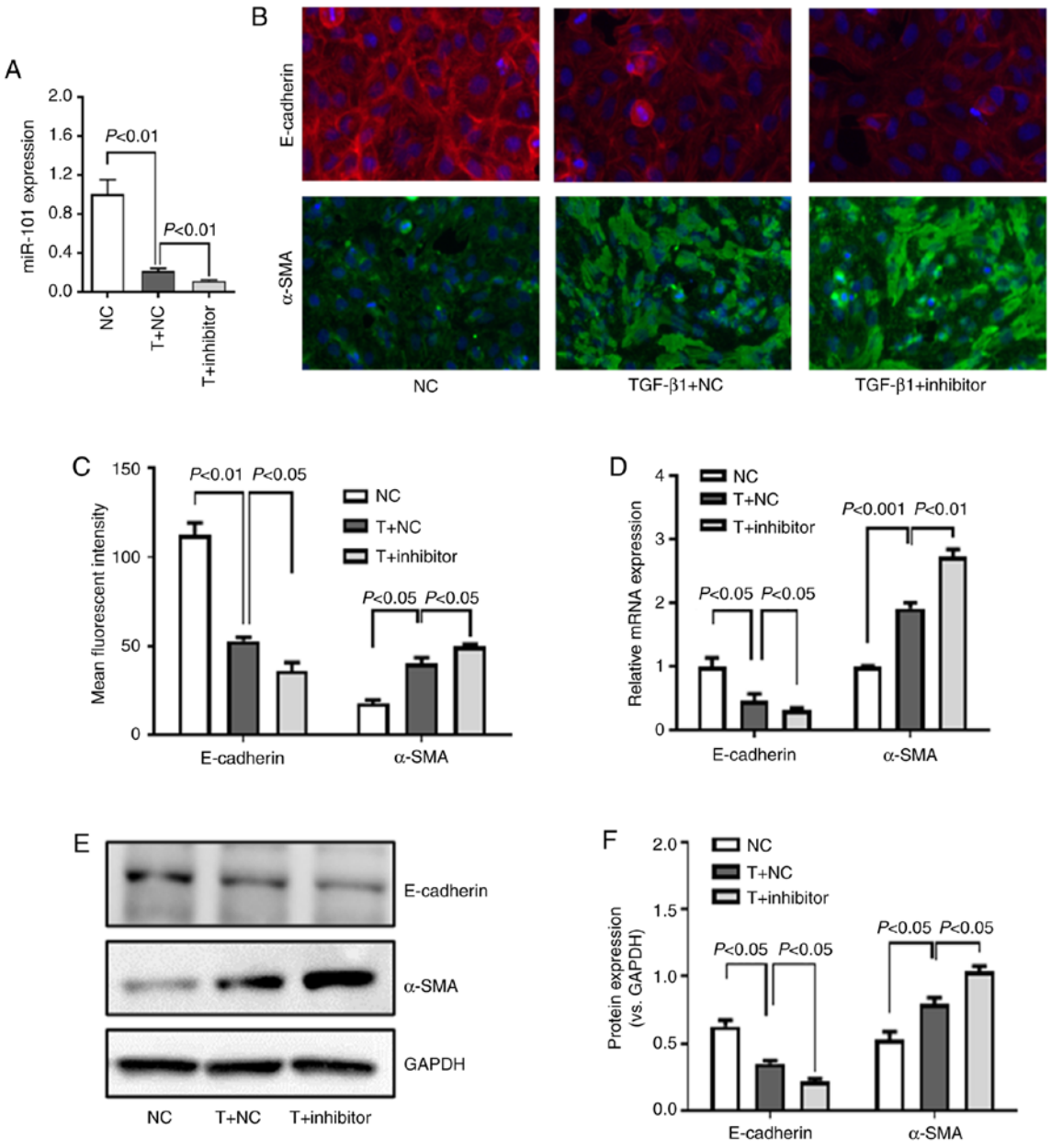

Figure 5. miR-101 inhibition enhances TGF-β1-induced EMT in HK-2 cells. A miR-101 inhibitor was transfected into HK-2 cells, which were then treated with TGF-β1, (A) and miR-101 expression was quantified. (B) E-cadherin and α-SMA expression as assessed by immunofluorescence. (C) E-cadherin and α-SMA staining intensity as quantified using the Thermo HCS StudioTM 2.0 Cell Analysis Program. (D) RT-qPCR was used to assess E-cadherin and α-SMA mRNA expression. (E) E-cadherin, and α-SMA levels in HK-2 cells were assessed by western blot analysis. (F) Densitometric quantification of the data in (D), with GAPDH used for normalization; NC, negative control; T, TGF-β1; inhibitor, miR-101 inhibitor; α-SMA, α-smooth muscle actin; TGF-β1, transforming growth factor-β1.

phosphorylation in HK-2 cells, suggesting that this miRNA can suppress TGF-β1/Smad3 signaling. Taken together, these findings demonstrate that miR-101 can control TβR-I expression so as to suppress TGF-β1 signaling.

To confirm these results, the cells were additionally treated with the potent TβR-I inhibitor, SB-431542. As was expected, SB-431542 suppressed TGF-β1 induced EMT in HK-2 cells. When cells were treated with this TβR-I inhibitor, the ability of miR-101 inhibition to impact EMT phenotypes was ablated, thus confirming that miR-101 ablates TGF-β1-induced EMT by directly targeting TβR-I. Recently, Zhao *et al* (42) also found that miR-101 inhibited acute kidney injury-chronic kidney disease transition by inhibiting the EMT process. The results of the present study revealed that miR-101 expression was downregulated in a rat renal fibrosis model, confirming that miR-101 may be important in different rodent renal diseases model. In an *in vitro* study, Zhao *et al* (42) found that miR-101 overexpression using miR-101 mimic inhibited EMT. Apart from the gain-of function experiment, in the present study, it was further confirmed that the downregulation of miR-101 using miR-101 inhibitor promoted the process of EMT. Taken together, the results further verified the key role of miR-101 in kidney diseases, and suggested that it may be a potential target for the treatment of renal fibrosis.

In conclusion, the findings of the present study highlight miR-101 as a key miRNA associated with $HgCl_2$-induced RIF.

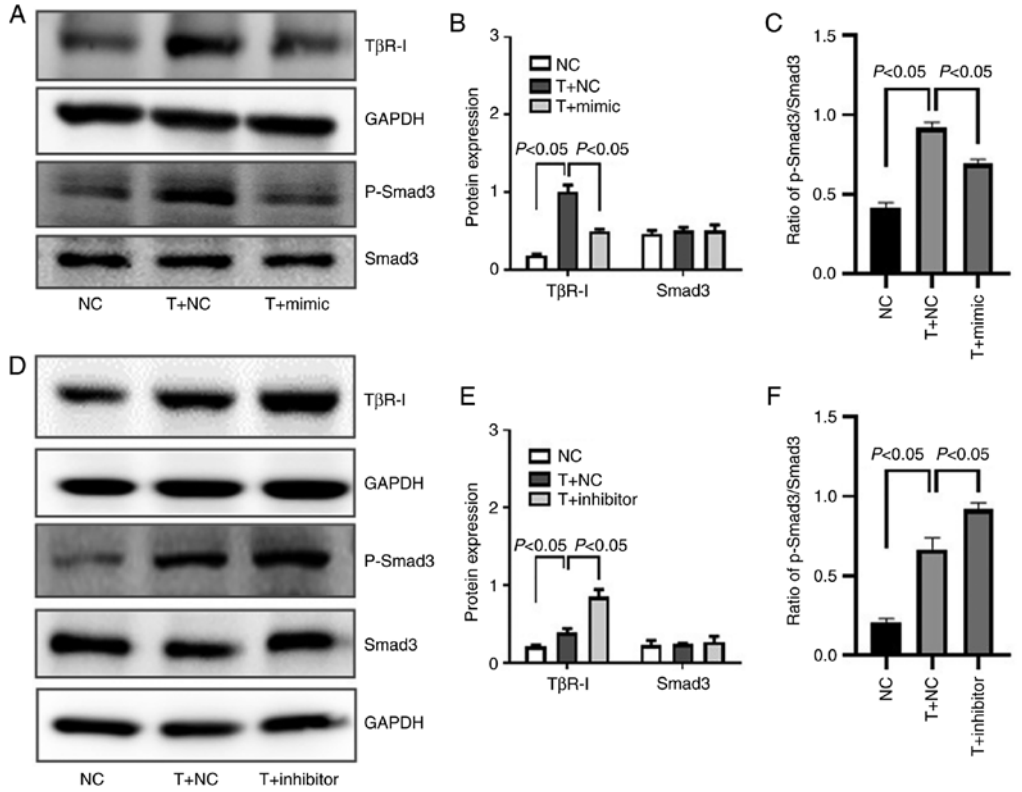

Figure 6. Effect of miR-101 on TβR-I and Smad3 in HK-2 cells. (A) TβR-I, Smad3 and p-Smad3 levels were assessed by western blot analysis in HK-2 cells following miR-101 mimic transfection. (B) Densitometric quantification of TβR-I and Smad3, with GAPDH being used for normalization. (C) Ratio of p-Smad3 vs. Smad3. (D) TβR-I, Smad3 and p-Smad3 levels were assessed by western blot analysis in HK-2 cells following miR-101 inhibitor transfection. (E) Densitometric quantification of TβR-I and Smad3, with GAPDH being used for normalization. (F) Ratio of p-Smad3 vs. Smad3. NC, negative control; T, TGF-β1; mimic, miR-101 mimic; inhibitor, miR-101 inhibitor; α-SMA, α-smooth muscle actin; TGF-β1, transforming growth factor-β1.

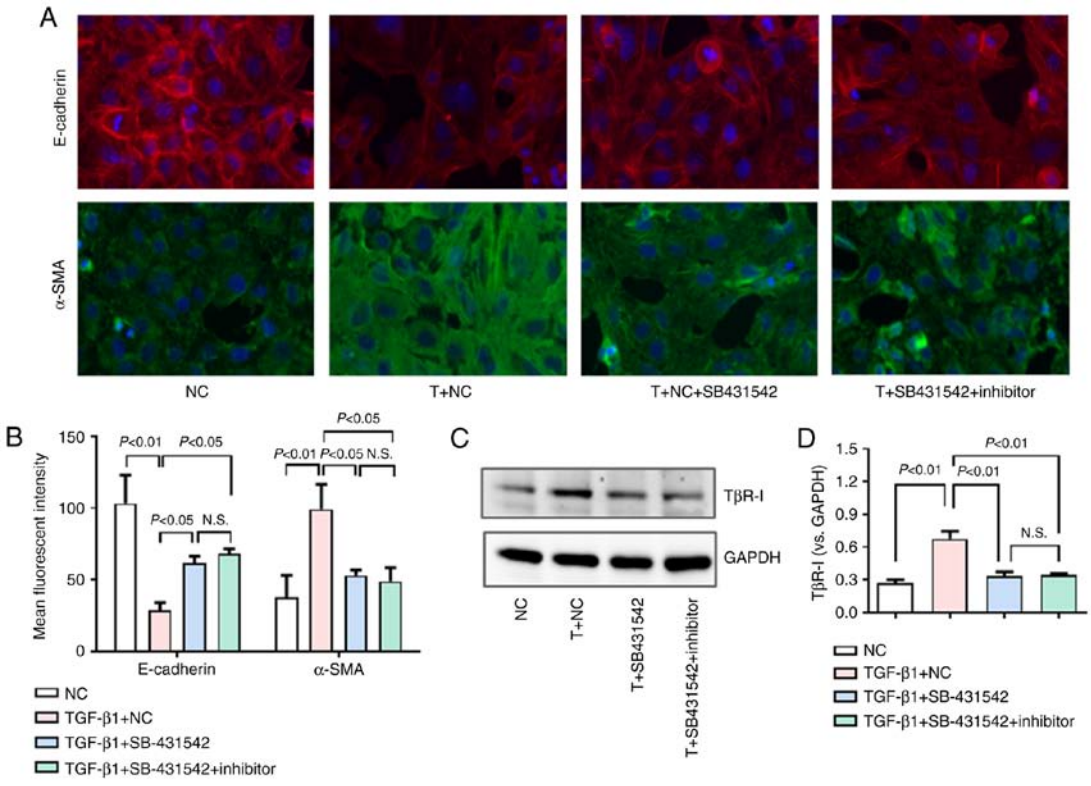

Figure 7. Effect of miR-101 inhibition on TβR-I inhibitor-treated HK-2 cells. (A) E-cadherin and α-SMA expression were assessed by immunofluorescence staining. (B) data in (A) were quantified using the Thermo HCS StudioTM 2.0 Cell Analysis Program. (C) TβR-I expression in HK-2 cells was assessed by western blot analysis. (D) Densitometric quantification of the data in (C), with GAPDH used for normalization. NC, negative control; T, TGF-β1; inhibitor, miR-101 inhibitor; α-SMA, α-smooth muscle actin; TGF-β1, transforming growth factor-β1.

It was found that this miRNA can suppress renal tubular EMT by targeting TβR-I and thereby inhibiting TGF-β1 signaling, thus indicating that miR-101 may be a viable target for treating RIF, although further research is required needed to confirm this hypothesis.

Acknowledgements

Not applicable.

Funding

The present study was supported by the National Natural Science Foundation of China (grant nos. 81573810 and 30901943), the China Postdoctoral Science Foundation (grant no. 2015T80445) and the National Science and Technology Major Project 'Key New Drug Creation and Manufacturing Program' of China (grant no. 2019ZX09201001).

Availability of data and materials

The datasets used and/or analyzed during the current study are available from the corresponding author on reasonable request.

Authors' contributions

PL, CL and QW conceived the study and established the initial design of the study. QW, YT and HX performed the experiments and analyzed the data. QW prepared the manuscript. All authors read and approved the final manuscript. QW and PL confirm the authenticity of all the raw data.

Ethics approval and consent to participate

The present study was approved by the Animal Research Ethics Committee of Shanghai University of Traditional Chinese Medicine, Shanghai, China.

Patient consent for publication

Not applicable.

Competing interests

The authors declare that they have no competing interests.

References

1. Farris AB and Colvin RB: Renal interstitial fibrosis: Mechanisms and evaluation. Curr Opin Nephrol Hypertens 21: 289-300, 2012.
2. Strutz F and Zeisberg M: Renal fibroblasts and myofibroblasts in chronic kidney disease. J Am Soc Nephrol 17: 2992-2998, 2006.
3. He L and Hannon GJ: MicroRNAs: Small RNAs with a big role in gene regulation. Nat Rev Genet 5: 522-531, 2004.
4. Fabian MR, Sonenberg N and Filipowicz W: Regulation of mRNA translation and stability by microRNAs. Annu Rev Biochem 79: 351-379, 2010.
5. Kloosterman WP and Plasterk RH: The diverse functions of microRNAs in animal development and disease. Dev Cell 11: 441-450, 2006.
6. Chung AC, Yu X and Lan HY: MicroRNA and nephropathy: Emerging concepts. Int J Nephrol Renovasc Dis 6: 169-179, 2013.
7. Yuan JL, Tao YY, Wang QL, Shen L and Liu CH: Fuzheng Huayu Formula () prevents rat renal interstitial fibrosis induced by HgCl2 via antioxidative stress and down-regulation of nuclear factor-kappa B activity. Chin J Integr Med 23: 598-604, 2017.
8. Wang QL, Tao YY, Yuan JL, Shen L and Liu CH: Salvianolic acid B prevents epithelial-to-mesenchymal transition through the TGF-beta1 signal transduction pathway in vivo and in vitro. BMC Cell Biol 11: 31, 2010.
9. Lei Y, Wang QL, Shen L, Tao YY and Liu CH: MicroRNA-101 suppresses liver fibrosis by downregulating PI3K/Akt/mTOR signaling pathway. Clin Res Hepatol Gastroenterol 43: 575-584, 2019.
10. Wang B, Yan Z, Li L, Wang Z and Liu H: Effect of MiR-101 on rats with CCl4-induced liver fibrosis through regulating Nrf2-ARE pathway. Panminerva Med: Jul 30, 2019 (Epub ahead of print).
11. Huang C, Xiao X, Yang Y, Mishra A, Liang Y, Zeng X, Yang X, Xu D, Blackburn MR, Henke CA and Liu L: MicroRNA-101 attenuates pulmonary fibrosis by inhibiting fibroblast proliferation and activation. J Biol Chem 292: 16420-16439, 2017.
12. Pan Z, Sun X, Shan H, Wang N, Wang J, Ren J, Feng S, Xie L, Lu C, Yuan Y, *et al*: MicroRNA-101 inhibited postinfarct cardiac fibrosis and improved left ventricular compliance via the FBJ osteosarcoma oncogene/transforming growth factor-β1 pathway. Circulation 126: 840-850, 2012.
13. Li X, Zhang S, Wa M, Liu Z and Hu S: MicroRNA-101 protects against cardiac remodeling following myocardial infarction via downregulation of runt-related transcription factor 1. J Am Heart Assoc 8: e013112, 2019.
14. Wang N, Duan L, Ding J, Cao Q, Qian S, Shen H and Qi J: MicroRNA-101 protects bladder of BOO from hypoxia-induced fibrosis by attenuating TGF-β-smad2/3 signaling. IUBMB Life 71: 235-243, 2019.
15. Viart V, Bergougnoux A, Bonini J, Varilh J, Chiron R, Tabary O, Molinari N, Claustres M and Taulan-Cadars M: Transcription factors and miRNAs that regulate fetal to adult CFTR expression change are new targets for cystic fibrosis. Eur Respir J 45: 116-128, 2015.
16. Liu Y: Cellular and molecular mechanisms of renal fibrosis. Nat Rev Nephrol 7: 684-696, 2011.
17. Yang J and Liu Y: Blockage of tubular epithelial to myofibroblast transition by hepatocyte growth factor prevents renal interstitial fibrosis. J Am Soc Nephrol 13: 96-107, 2002.
18. Allison SJ: Fibrosis: Targeting EMT to reverse renal fibrosis. Nat Rev Nephrol 11: 565, 2015.
19. Loeffler I and Wolf G: Transforming growth factor-beta and the progression of renal disease. Nephrol Dial Transplant 29 (Suppl 1): i37-i45, 2014.
20. Iwano M: EMT and TGF-beta in renal fibrosis. Front Biosci (Schol Ed) 2: 229-238, 2010.
21. Zhao X, Wang K, Liao Y, Zeng Q, Li Y, Hu F, Liu Y, Meng K, Qian C, Zhang Q, *et al*: MicroRNA-101a inhibits cardiac fibrosis induced by hypoxia via targeting TGFβRI on cardiac fibroblasts. Cell Physiol Biochem 35: 213-226, 2015.
22. Close B, Banister K, Baumans V, Bernoth EM, Bromage N, Bunyan J, Erhardt W, Flecknell P, Gregory N, Hackbarth H, *et al*: Recommendations for euthanasia of experimental animals: Part 1. DGXI of the European commission. Lab Anim 30: 293-316, 1996.
23. Jamall IS, Finelli VN and Que Hee SS: A simple method to determine nanogram levels of 4-hydroxyproline in biological tissues. Anal Biochem 112: 70-75, 1981.
24. Smyth GK: Linear models and empirical bayes methods for assessing differential expression in microarray experiments. Stat Appl Genet Mol Biol 3: Article3, 2004.
25. Joung JG, Hwang KB, Nam JW, Kim SJ and Zhang BT: Discovery of microRNA-mRNA modules via population-based probabilistic learning. Bioinformatics 23: 1141-1147, 2007.
26. Livak KJ and Schmittgen TD: Analysis of relative gene expression data using real-time quantitative PCR and the 2(-Delta Delta C(T)) method. Methods 25: 402-408, 2001.
27. Iwano M, Plieth D, Danoff TM, Xue C, Okada H and Neilson EG: Evidence that fibroblasts derive from epithelium during tissue fibrosis. J Clin Invest 110: 341-350, 2002.
28. Tu X, Zhang H, Zhang J, Zhao S, Zheng X, Zhang Z, Zhu J, Chen J, Dong L, Zang Y and Zhang J: MicroRNA-101 suppresses liver fibrosis by targeting the TGFβ signalling pathway. J Pathol 234: 46-59, 2014.
29. Meng XM, Chung AC and Lan HY: Role of the TGF-β/BMP-7/Smad pathways in renal diseases. Clin Sci (Lond) 124: 243-254, 2013.

30. Chaudhary NI, Roth GJ, Hilberg F, Müller-Quernheim J, Prasse A, Zissel G, Schnapp A and Park JE: Inhibition of PDGF, VEGF and FGF signalling attenuates fibrosis. Eur Respir J 29: 976-985, 2007.
31. Rudnicki M, Perco P, D Haene B, Leierer J, Heinzel A, Mühlberger I, Schweibert N, Sunzenauer J, Regele H, Kronbichler A, *et al*: Renal microRNA- and RNA-profiles in progressive chronic kidney disease. Eur J Clin Invest 46: 213-226, 2016.
32. Wang QL, Yuan JL, Tao YY, Zhang Y, Liu P and Liu CH: Fuzheng Huayu recipe and vitamin E reverse renal interstitial fibrosis through counteracting TGF-beta1-induced epithelial-to-mesenchymal transition. J Ethnopharmacol 127: 631-640, 2010.
33. Hou X, Tian J, Geng J, Li X, Tang X, Zhang J and Bai X: MicroRNA-27a promotes renal tubulointerstitial fibrosis via suppressing PPARγ pathway in diabetic nephropathy. Oncotarget 7: 47760-47776, 2016.
34. Liu Y, Bi X, Xiong J, Han W, Xiao T, Xu X, Yang K, Liu C, Jiang W, He T, *et al*: MicroRNA-34a promotes renal fibrosis by downregulation of klotho in tubular epithelial cells. Mol Ther 27: 1051-1065, 2019.
35. Li H, Xu Y, Zhang Q, Xu H, Xu Y and Ling K: Microvesicles containing miR-34a induce apoptosis of proximal tubular epithelial cells and participate in renal interstitial fibrosis. Exp Ther Med 17: 2310-2316, 2019.
36. Denby L, Ramdas V, Lu R, Conway BR, Grant JS, Dickinson B, Aurora AB, McClure JD, Kipgen D, Delles C, *et al*: MicroRNA-214 antagonism protects against renal fibrosis. J Am Soc Nephrol 25: 65-80, 2014.
37. Zhang J, Jiao J, Cermelli S, Muir K, Jung KH, Zou R, Rashid A, Gagea M, Zabludoff S, Kalluri R and Beretta L: miR-21 inhibition reduces liver fibrosis and prevents tumor development by inducing apoptosis of $CD24^+$ progenitor cells. Cancer Res 75: 1859-1867, 2015.
38. McClelland AD, Herman-Edelstein M, Komers R, Jha JC, Winbanks CE, Hagiwara S, Gregorevic P, Kantharidis P and Cooper ME: miR-21 promotes renal fibrosis in diabetic nephropathy by targeting PTEN and SMAD7. Clin Sci (Lond) 129: 1237-1249, 2015.
39. Yuan J, Chen H, Ge D, Xu Y, Xu H, Yang Y, Gu M, Zhou Y, Zhu J, Ge T, *et al*: Mir-21 promotes cardiac fibrosis after myocardial infarction via targeting Smad7. Cell Physiol Biochem 42: 2207-2219, 2017.
40. Carew RM, Wang B and Kantharidis P: The role of EMT in renal fibrosis. Cell Tissue Res 347: 103-116, 2012.
41. Xu J, Lamouille S and Derynck R: TGF-beta-induced epithelial to mesenchymal transition. Cell Res 19: 156-172, 2009.
42. Zhao JY, Wang XL, Yang YC, Zhang B and Wu YB: Upregulated miR-101 inhibits acute kidney injury-chronic kidney disease transition by regulating epithelial-mesenchymal transition. Hum Exp Toxicol 39: 1628-1638, 2020.